

TURBULENT FLOWS OVER ROUGH WALLS

Javier Jiménez

*School of Aeronautics, U. Politécnica Madrid, 28040 Madrid, Spain;
Center for Turbulence Research, Stanford University, Stanford, California 94305;
e-mail: jimenez@torroja.dmt.upm.es*

Key Words turbulence, roughness

■ **Abstract** We review the experimental evidence on turbulent flows over rough walls. Two parameters are important: the roughness Reynolds number k_s^+ , which measures the effect of the roughness on the buffer layer, and the ratio of the boundary layer thickness to the roughness height, which determines whether a logarithmic layer survives. The behavior of transitionally rough surfaces with low k_s^+ depends a lot on their geometry. Riblets and other drag-reducing cases belong to this regime. In flows with $\delta/k \lesssim 50$, the effect of the roughness extends across the boundary layer, and is also variable. There is little left of the original wall-flow dynamics in these flows, which can perhaps be better described as flows over obstacles. We also review the evidence for the phenomenon of d -roughness. The theoretical arguments are sound, but the experimental evidence is inconclusive. Finally, we discuss some ideas on how rough walls can be modeled without the detailed computation of the flow around the roughness elements themselves.

1. INTRODUCTION

Turbulent flows over rough walls have been studied since the early works of Hagen (1854) and Darcy (1857), who were concerned with pressure losses in water conduits. They have been important in the history of turbulence. Had those conduits not been fully rough, turbulence theory would probably have developed more slowly. The pressure loss in pipes only becomes independent of viscosity in the fully rough limit, and this independence was the original indication that something was amiss with laminar theory. Flows over smooth walls never become fully turbulent, and their theory is correspondingly harder.

Most turbulence textbooks include material on roughness, and the one by Schlichting (1968, Ch. 20 and 21) is still a useful reference. A more recent review is the one by Raupach et al. (1991). The related field of flows over plant canopies has been summarized by Raupach & Tom (1981) and more recently by Finnigan (2000).

There is an extensive literature on the atmospheric boundary layer, which is almost always rough, although much of it deals with other effects besides roughness,

such as stratification and rotation. Geophysical flows are beyond our scope, but we occasionally compare them with the high Reynolds number limit of industrial or laboratory ones. Older reviews such as those by Monin (1970) and Counihan (1975) are most useful for that purpose because they tend to focus on the adiabatic atmospheric boundary, for which roughness is the dominant effect near the ground.

Much of the literature before 1990 concerns itself with the universal aspects of flows over rough walls; more recent research has emphasized the differences between different types of roughness. It has been suggested that the details of the wall may influence the flow across the whole boundary layer, and part of this review is dedicated to sorting those claims and their significance in understanding wall turbulence. Because of space limitations we restrict ourselves to the fluid dynamics of fully turbulent flows over rough walls, neglecting other important topics. One of them is transition, which can be promoted (Schlichting 1968, pp. 509–15) or delayed by roughness (Wassermann & Kloker 2002). Another one is the role of roughness in enhancing heat transfer, recently reviewed by Kalinin & Dreitzer (1998), which is a field by itself.

The structure of the article is as follows. After a short summary of the theory of flows over smooth walls, which sets the stage for later discussions, we review the effect on the mean flow in Section 2, and we treat the structure of the turbulent fluctuations in Section 3. We briefly discuss theoretical models in Section 4, which is followed by closing considerations. We use x , y , and z for the streamwise, wall-normal, and spanwise coordinates, and u , v , and w for the corresponding velocity components. The time-averaged value of the streamwise velocity is denoted by U , and primed variables such as u' represent the root-mean-squared values of fluctuating quantities. We use δ for either the 99% boundary-layer thickness, for the pipe radius, or for the channel half-width, and reserve U_δ for the centerline or for the free-stream velocity.

1.1. The Overall Structure of Wall-Bounded Flows

The overall structure of turbulent boundary layers over smooth walls can be found in classical textbooks (Townsend 1976). Wall flows are governed by two sets of scales whose influence is stratified in terms of the wall distance. Near the wall viscosity is important and the relevant scaling parameters are the friction velocity $u_\tau = (\tau/\rho)^{1/2}$, where τ and ρ are the tangential wall stress and the fluid density, and the kinematic viscosity ν . From them we can construct a viscous length scale ν/u_τ . Quantities normalized in these wall units are identified by a $+$ superindex. The thin-layer approximation to the momentum equation implies that the order of magnitude of the Reynolds stresses is u_τ^2 across the boundary layer, and u_τ acts as a global velocity scale.

Viscosity is dominant below $y^+ \approx 5$, and the most active part of the flow is the buffer region between $10 \leq y^+ \leq 100$. This layer is home to a nonlinear self-sustaining cycle (Jiménez & Moin 1991), which is responsible for generating most of the turbulent energy in moderate Reynolds number flows. Its mechanics

have been essentially clarified in the last decade (Hamilton et al. 1995, Jiménez & Pinelli 1999). It involves long longitudinal streaks of high and low streamwise velocity, and shorter quasi-streamwise vortices (Robinson 1991).

At distances from the wall of the order of boundary-layer thickness, the size of the structures is limited by δ , which becomes the relevant length scale. The Reynolds number $\delta^+ = \delta u_\tau / \nu$ defines the scale separation between the outer and inner lengths. If δ^+ is large enough, between the outer region and the buffer layer there is an overlap layer in which y^+ is too large for viscosity to be important and y/δ is too small for δ to be relevant. The only available length scale is then the wall distance, leading to a logarithmic distribution of the mean streamwise velocity (Townsend 1976),

$$U^+(y) = \kappa^{-1} \log y^+ + A. \quad (1)$$

The Kármán constant, $\kappa \approx 0.4$, depends only on the properties of the overlap layer and is believed to be universal. The additive constant A is determined by the no-slip boundary condition at the wall but, because Equation 1 is only valid for $y^+ \gg 1$, its value depends on the details of the buffer and viscous layers. For smooth walls its experimental value is $A \approx 5.1$.

A composite velocity profile valid above $y^+ \gtrsim 50$ is often written as

$$U^+(y) = \kappa^{-1} \log y^+ + A + \Pi \kappa^{-1} W(y/\delta), \quad (2)$$

where the “wake” component W represents the effect of the outer-layer dynamics. Its form depends on the external driving mechanism for the boundary layer, but it is typically negligible below $y/\delta \approx 0.15$, which is considered the upper limit of the logarithmic layer. The wake function is conventionally normalized to $W(1) = 2$, and $2\Pi/\kappa$ measures the contribution of the outer-layer structures to the mean velocity profile, in the same way that A measures the influence of the near-wall layer. For zero-pressure-gradient boundary layers, and for pipes and channels, Π is at most of order unity. This implies that the logarithmic layer where Equation 1 is valid sustains between 70% and 80% of the total velocity difference across the boundary layer, and is responsible for at least half of the overall production of turbulent energy. Those fractions increase with increasing δ^+ .

If the height k of the roughness elements is larger than a few wall units, roughness modifies this picture by interfering with the operation of the buffer-layer viscous cycle, and by completely destroying it when $k^+ \gtrsim 50$ –100. The main effect is to change the additive constant A but, because most of the turbulent energy is generated within the logarithmic layer, roughness may also modify the whole flow if k is not negligible with respect to δ . For example, if we admit that the direct effect of the roughness elements extends to 2 – $3k$, we would need $\delta/k > 40$ for the roughness to directly affect less than half of the thickness of the logarithmic layer.

Because of the logarithmic form of Equation 2, the friction velocity depends weakly on δ^+ . In most wall-bounded flows without strong pressure gradients $U_\delta/u_\tau \approx 20$ –30, and the viscous length scale depends almost exclusively on

the flow velocity and on the viscosity, not on the Reynolds number. For industrial flows in water at $U_\delta = 1\text{--}10$ m/s, or for air at $U_\delta = 30\text{--}300$ m/s, the viscous length is approximately $2\text{--}20\ \mu\text{m}$. The root-mean-squared roughness of machined surfaces ranges from $0.05\ \mu\text{m}$ to $25\ \mu\text{m}$ (Hutchings 1992), making most clean industrial surfaces hydrodynamically smooth or at most transitionally rough. For most industrial applications except heat exchangers $\delta/k \gg 1$, and the classical structure described above applies.

Virtually all surfaces of geophysical or meteorological interest are rough. The characteristic height of the roughness elements in natural terrains ranges from a few microns in the case of snow and fresh mud, to several centimeters in open rural terrain, and to tens of meters over forests and cities (Monin 1970). The thickness of the atmospheric boundary layer is $\delta \approx 500$ m (Counihan 1975), so that the ratio δ/k is large in open rural areas, but not necessarily so over cities or forests (Chen & Castro 2002).

Besides the obvious effects of roughness just discussed there are subtler possibilities. Researchers have known for some time that structures with outer length scales penetrate into the buffer region (Hites 1997, Del Álamo & Jiménez 2003), and it has also been suggested that those outer-layer structures grow from “hairpin” eddies generated near the wall (Head & Bandyopadhyay 1981, Adrian et al. 2000). It is therefore possible that at least some rough walls may influence the whole layer by modifying the form of the hairpins (Bandyopadhyay & Watson 1988), and the behavior of the roughness layer in other cases may be directly modified by events coming from the outside. Both mechanisms have been proposed.

2. THE MEAN FLOW

The most important effect of roughness is the previously mentioned change of the mean velocity profile near the wall, with the consequent modification of the friction coefficient. The best known early experiments on this aspect are the ones by Nikuradse (1933), who studied pipes roughened with carefully graded, closely packed sand. He found that the logarithmic velocity distribution for the mean velocity profile could still be used in the wall layer, with the same value of the Kármán constant as over smooth walls, and he expressed the velocity profile as

$$U^+(y) = \kappa^{-1} \log(y/k_s) + 8.5 + \Pi\kappa^{-1}W(y/\delta). \quad (3)$$

This equation has become the definition of the “equivalent” or “effective” sand roughness k_s . Over rough walls there is a question of which origin to use for y . The shift Δy from some reference location is usually determined empirically to maximize the quality of the logarithmic fit in Equation 3, and is typically some fraction of k . Raupach et al. (1991) thoroughly discuss this issue, which is important for interpreting experimental results.

An alternative way of expressing Equation 3 is

$$U^+(y) = \kappa^{-1} \log y^+ + 5.1 + \Pi\kappa^{-1}W(y/\delta) - \Delta U^+, \quad (4)$$

where the first three terms form the expression for a smooth wall, and the last one is an offset usually called the roughness function. Still another expression is

$$U^+ = \kappa^{-1} \log(y/k_0) + \Pi \kappa^{-1} W(y/\delta), \quad (5)$$

where $k_0 = 0.033k_s$ is called the roughness length. The three quantities k_s^+ , ΔU^+ , and k_0^+ characterize roughness interchangeably. The first one is most often used in engineering applications, the second one in wind-tunnel research, and the last one in geophysics. Comparing Equation 3 with Equation 4 links the three definitions.

Note that, even if in Nikuradse's case k_s is the grain size of the sand, it is in general only a convenient way of characterizing the drag increment due to the roughness. Consider the skin friction generated by two boundary layers, one rough and the other one smooth, with identical mean velocities U at a given location y within the logarithmic layer. In the smooth and rough cases Equation 4 can be written as

$$U_\ell^+ + \kappa^{-1} \log U_\ell^+ = \kappa^{-1} \log R + 5.1 = B_\ell, \quad (6)$$

and

$$U_r^+ + \kappa^{-1} \log U_r^+ = \kappa^{-1} \log (R/k_s^+) + 8.5 = B_r, \quad (7)$$

where $R = Uy/\nu$, and the subindices ℓ and r refer to smooth and rough values. These two equations have to be solved for $U^+ = U/u_\tau$, and higher values of U^+ imply lower skin frictions. They both have the same form with different right-hand sides B . It is easy to check that U^+ is a monotonically increasing function of B , so that the difference in wall drag between smooth and rough walls is controlled by the difference

$$B_\ell - B_r = \kappa^{-1} \log k_s^+ - 3.4. \quad (8)$$

For $k_s^+ \lesssim 4$ the skin friction of the rough wall would be less than that of the smooth one. There is no obvious reason why this should not be the case, but the opposite is usually true. Roughness elements seem to be more efficient generators of skin friction than smooth walls, presumably because they generate more turbulent dissipation than the relatively delicate viscous cycle. This is not an absolute rule, and some moderately rough surfaces reduce drag (Tani 1988, Sirovich & Karlsson 1997, Bechert et al. 2000). A well-documented example is the flow over riblets, which are narrow grooves aligned with the mean flow. They decrease drag by up to 10% (Walsh 1990), and are discussed below. In most cases $k_s^+ \approx 4$ is however a lower limit below which the drag is the same as over a smooth wall.

In the limit $B_\ell \gg B_r$ the viscous component of the skin friction is negligible compared with the drag of the roughness elements, and the flow becomes asymptotically independent of viscosity. In this limit

$$\frac{u_{\tau,r}}{u_{\tau,\ell}} \approx \frac{B_\ell}{B_r}, \quad (9)$$

so that to have a skin friction larger than twice that of a smooth wall we need $B_r \lesssim B_\ell/\sqrt{2}$. Because B_ℓ is approximately 20–30 in the logarithmic layer, this implies $B_\ell - B_r \gtrsim 7.5$ and $k_s^+ \gtrsim 80$. In practice k_s/k becomes independent of k_s^+ around that threshold, beyond which the flow is considered fully rough.

We stress that the previous argument deals with the drag properties of the flow, and that the equivalent sand roughness is a hydrodynamic concept that needs to be related to the surface geometry before it can be used.

2.1. ‘ K ’-Roughness

Dimensional analysis suggests that in the limit in which $k^+ \gg 1$ and viscosity becomes irrelevant, k_s should be proportional to the dimensions of the roughness elements. The “normal” surfaces for which this is true are called k -rough, to distinguish them from the d -roughness described below. The ratio k_s/k depends on the geometry of the roughness, and particularly on its surface density, which was quantified by Schlichting (1936) by the solidity λ , which is the total projected frontal roughness area per unit wall-parallel projected area. He performed a fairly complete set of experiments designed to test this effect, which are still often used to test theories and empirical correlations. They are presented, together with a few others, in Figure 1*a*. There are two regimes: the sparse one below $\lambda \approx 0.15$, for which the effect of the roughness increases with the solidity, and the dense one for which it decreases because the roughness elements shelter each other. In the sparse region it is intuitively clear that the extra roughness drag should be proportional to the frontal surface of the roughness elements, and $k_s/k \sim \lambda$. Much of the scatter of the original experiments in that range can be accounted for by scaling the drag of each surface by an appropriate drag coefficient of the individual elements. Following Tillman (1944), we use $c_D \approx 1.25$ for two-dimensional spanwise obstacles, and $c_D \approx 0.15$ – 0.3 for three-dimensional rounded ones.

A re-evaluation of Schlichting’s results was published by Coleman et al. (1984), and has occasionally been used instead of the original experiments. The differences are only significant for very sparse roughness, and they are used in Figure 1*a* to compute the error bars.

The solidity has often been used for engineering correlations, but it cannot by itself fully characterize a surface. For example, the mutual sheltering of the roughness elements depends on other geometric factors, and correlations such as those in Figure 1*a* apply only to particular sets of experiments. There is not even a qualitative theory for the power of λ , which should describe the dense regime. Figure 1*a* uses λ^{-2} , which is close to some engineering correlations, but powers down to λ^{-5} have been proposed (Dvorak 1969). There have been many attempts to improve the empirical correlations by choosing better parameters to describe the surface (Simpson 1973, Bandyopadhyay 1987). Waigh & Kind’s (1998) is a particularly complete compilation.

Most correlations are restricted to surfaces whose geometry is easily described, and cannot easily cope with irregular surfaces that are often only known by

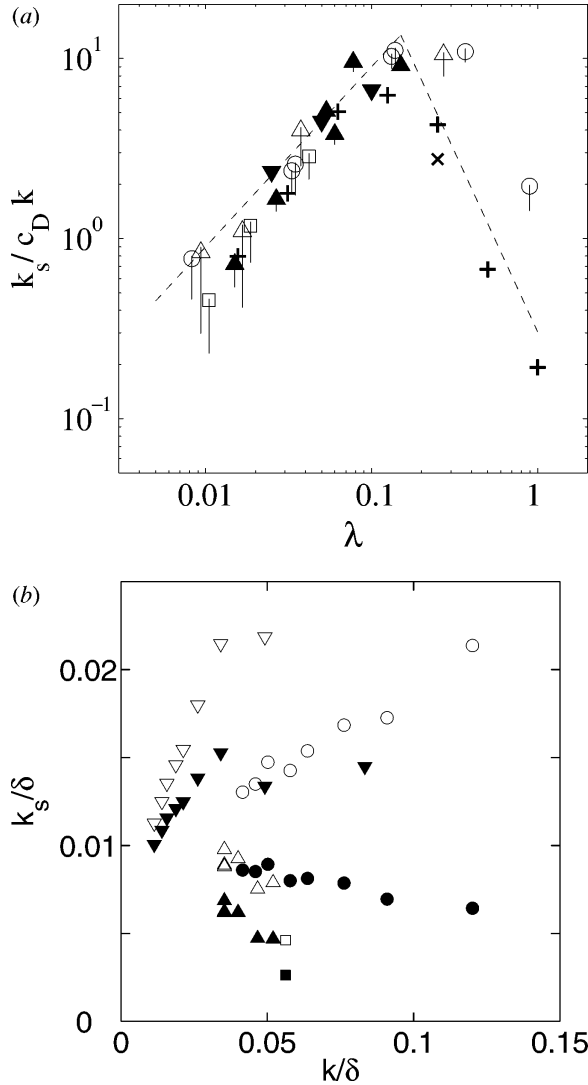


Figure 1 (a) Equivalent sand roughness for various k -surfaces versus the solidity λ , corrected with empirical drag coefficients. Open symbols, rounded elements (spheres, cones, $c_D = 0.3$; spherical segments, $c_D = 0.13$) from Schlichting (1936). For all others, $c_D = 1.25$. \blacktriangle , spanwise fences (Schlichting 1936); \blacktriangledown , spanwise fences (Webb et al. 1971); $+$, spanwise cylinders (Tani 1987); \times , spanwise square bars (Bandyopadhyay 1987). The dashed lines have logarithmic slopes $+1$ and -2 . For the error bars, see text. (b) Equivalent sand roughness for d -type walls, versus k/δ . \triangle , Wood & Antonia (1975); \circ , Perry et al. (1969); ∇ , Bandyopadhyay (1987); \square , Tani (1987). The solid symbols are corrected for the effect of k/δ , following Simpson (1973).

their mode of preparation. Townsin (1991) attempted to correlate the drag of such surfaces with the moments of the spectra of the roughness height while analyzing surfaces of interest in naval construction, and Raupauch et al. (1991) gave empirical correlations for plant canopies. Taylor et al. (1995) pioneered an approach in which the flow in the layer below the roughness top is approximated by a series of two-dimensional wall-parallel slices, computing the drag in each of them using a turbulence model. They had some success in the *ab initio* determination of the drag characteristics of sparse roughness (Scraggs et al. 1988).

2.2. 'D'-Roughness

The distinction between *d*- and *k*-roughness was first made by Perry et al. (1969), who also summarized previous evidence for *d*-type behavior. They observed that, in several boundary layers over plates that had been roughened by narrow spanwise square grooves, the effective roughness k_s was not proportional to the roughness height (the *k*), but to the boundary-layer thickness (the *d*),

$$k_s \approx 0.02\delta. \quad (10)$$

This result has to be taken with care because it was only documented for a single zero-pressure-gradient case in which the ratio of the boundary layer thickness to the groove depth was 10–20, and where asymptotic scaling laws should not be expected.

This criticism is not valid for their adverse-pressure-gradient boundary layers, which were thicker, but the only correlation in those cases was that k_s was proportional to the offset Δy of the logarithmic layer's origin with respect to the top of the grooves, which could not be related to other physical lengths. It is nevertheless interesting that the value of Δy measured at the downstream end of some boundary layers was twice larger than either the groove width or the depth.

Figure 1*b* shows a compilation of effective roughness heights for *d*-surfaces, and only partially supports the conclusion that the effective roughness is independent of the roughness dimensions. In the individual experiments, represented by open symbols, k_s is not proportional to *k*, but neither is the overall picture consistent with a constant value for k_s/δ . The problem is in part the narrow range of k/δ in each experiment, but also that in most cases k/δ is relatively large. Only Bandyopadhyay's (1987) experiments satisfy the criterion set in the introduction that $\delta/k > 40$, and they are also the ones that behave less like *d*-walls. Simpson (1973) studied the effect of k/δ on the drag of a particular *k*-surface, and suggested that

$$\Delta_0 U^+ \approx \Delta U^+ - 25 k/\delta, \quad (11)$$

where $\Delta_0 U^+$ would be an ideal value at $k/\delta = 0$. That correction has been applied to the solid symbols in Figure 1*b*, and the resulting values are in somewhat better agreement with *d*-behavior, but the magnitude of the correction suggests that there

is a need for a definitive set of experiments with emphasis on sufficiently high values of both δ/k and k^+ .

Even with these uncertainties d -roughness has been studied extensively, both because it is difficult to understand how the origin of the logarithmic layer could be offset by more than the physical roughness dimensions, and because it promises a way of constructing boundary layers with a single length scale. Because much of the complication of wall-bounded flows is due to the interplay between two independent length scales, the proportionality in Equation 10 implies that d -type layers have only outer scales and are, in a sense, pure core flows.

The grooves in d -type walls are roughly square, with a solidity $\lambda \approx 0.5$, which is in the limit of extreme mutual sheltering in Figure 1a. The usual explanation for their behavior is that they sustain stable recirculation vortices that isolate the outer flow from the roughness (Figure 2). Walls with grooves wider than $3-4k$ behave like k -type surfaces, and also have recirculation bubbles that reattach ahead of the next rib, exposing it to the outer flow. Perry et al. (1969) explicitly observed the difference in recirculation lengths, and Djenidi et al. (1994) and Liou et al. (1990) confirmed it in flow visualizations of individual grooves.

Although this model explains how the flow becomes isolated from the interior of the grooves, making k_s independent of their depth, the role of the boundary-layer thickness is harder to understand. In the limit of ideally stable groove vortices, the outer flow sees a boundary condition that alternates between no slip at the rib tops and partial slip over the cavities, and the relevant length scales would seem to be the groove width and pitch, both of which are proportional to k . To get around this difficulty, it has been proposed that groups of grooves occasionally eject their vorticity into the wall layer, and that these ejections are triggered by large-scale sweeps originating in the outer flow (Townsend 1976, p. 142). There has been a lot of discussion on whether the outer flow structures couple directly with near-wall events, with various investigators finding that the periods between buffer-layer “bursts” over smooth walls scale in outer units (Laufer & Narayanan 1971), inner units (Luchik & Tiederman 1987), or their geometric mean

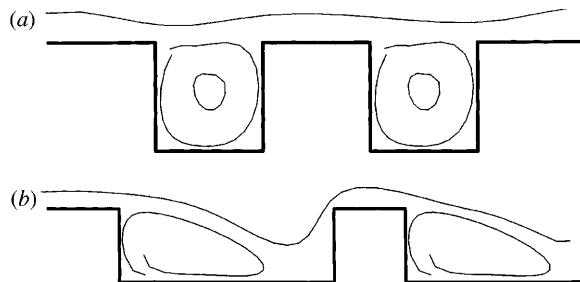


Figure 2 Geometry of (a) d -type, and (b) k -type slotted walls. Flow is from left to right.

(Shah & Antonia 1989). A full discussion is beyond this review, but it is conceivable that a length scale δ could arise from those interactions.

Djenidi et al. (1994) visualized ejections from individual groove vortices under turbulent boundary layers, and Taniguchi & Evans (1993) gave evidence of their modulation by passing turbulence. Ghaddar et al. (1986a) analyzed the simpler system of a grooved laminar channel and found that the vortices bifurcate spontaneously to an oscillatory state at fairly low Reynolds numbers and that the bifurcation eventually leads to subharmonic behavior in which several grooves eject collectively. Ghaddar et al. (1986b) later enhanced the heat transfer in the channel by pulsating the flow at frequencies resonating with the natural instability, supporting the idea that similar resonances could occur naturally over d -type surfaces.

2.3. Transitional Roughness

The flow regime in which k^+ is not large enough for a fully rough behavior is, somewhat confusingly, called “transitionally” rough. The name has nothing to do with transition to turbulence, which is controlled by δ^+ .

Transitional roughness functions for several surfaces are collected in Figure 3, but it is important to realize that the Reynolds number used in the abscissae is not based on the equivalent sand roughness k_s . We saw at the beginning of the section that k_s^+ is a flow property that univocally determines ΔU^+ . What is done in practice, and what is done in Figure 3, is to assign to each surface a single “geometric” sand roughness, which is the fixed value that corresponds to its skin friction in the fully rough regime at high Reynolds numbers. This geometric roughness $k_{s\infty}$ is a property of the surface, and can be used to characterize the Reynolds number of the flow. It guarantees the collapse of all the roughness functions in the fully rough regime. Nikuradse (1933) observed that, for graded sand, the roughness function vanishes at $k_{s\infty}^+ \approx 4$, which has often been incorrectly quoted as meaning that all surfaces below $k^+ = 4$ are hydrodynamically smooth.

Colebrook (1939) collected results for several industrial pipes and found more gradual transitions, also included in Figure 3. His results depend on the particular surface, but to simplify their practical use, he proposed a “universal” interpolation formula¹

$$\Delta U^+ = \kappa^{-1} \log \left(1 + 0.26k_{s\infty}^+ \right), \quad (12)$$

which Moody (1944) later used to compute his commonly used skin-friction diagram for pipes. The discrepancy between the two results was already noted by Schlichting (1968), but became lost in practice. Surfaces below $k^+ \approx 4$ are still often considered “smooth,” whereas engineers use Moody’s more gradual formula.

¹Note that this formula is incorrectly used for uniform sand roughness in the book by White (1991, p. 427).

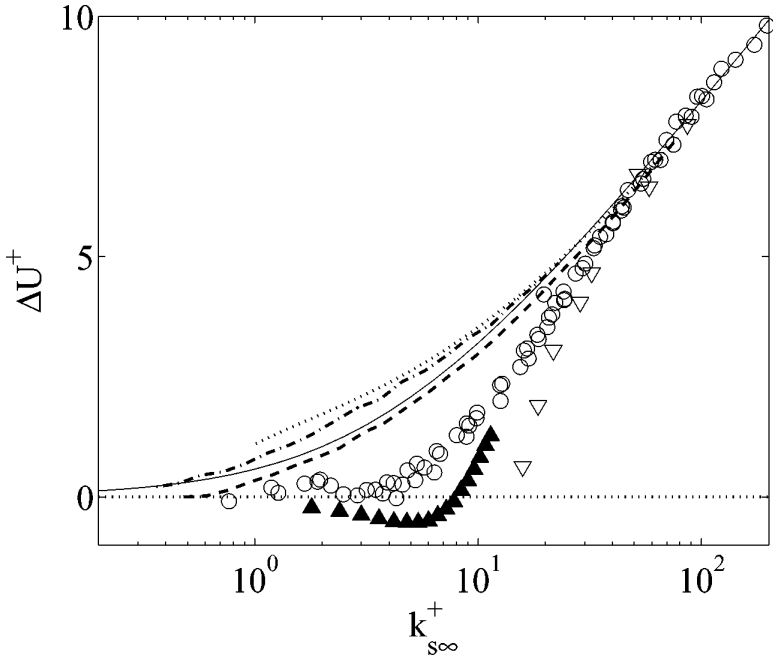


Figure 3 Roughness function for several transitionally rough surfaces, as a function of the Reynolds number based on the fully rough equivalent sand roughness. \circ , uniform sand (Nikuradse 1933); ∇ , uniform packed spheres (Ligrani & Moffat 1986); \blacktriangle , triangular riblets (Bechert et al. 1997); \cdots , galvanized iron; $---$, tar-coated cast iron; $- \cdot -$, wrought-iron (Colebrook 1939); $---$, Equation 12.

Bradshaw (2000) revived the question, noting that a minimum transitional height was unlikely for sparse roughness because the drag of the roughness elements in a shear is proportional to k^2 even in the low Reynolds number limit, and this should be reflected in ΔU^+ . In recent years the matter has become topical because some of the experiments undertaken to clarify the high Reynolds number behavior of flows over smooth walls have surfaces that would be hydrodynamically smooth or rough depending on which criterion is used (Barenblatt & Chorin 1998, Perry et al. 2001). Figure 3 shows that there is no “true” answer, and that each surface has to be treated individually.

The solid symbols in Figure 3 correspond to triangular riblets measured by Bechert et al. (1997). The drag-reducing property of streamwise-aligned riblets is a transitional roughness effect (Tani 1988). When they exceed $k^+ \approx 10$ they lose effectiveness, and their behavior when $k^+ \gg 1$ is that of regular k -surfaces. Their drag-reducing mechanism is reasonably well understood. Luchini, Manzo & Pozzi (1991) showed that, in the limit $k^+ \ll 1$, the effect of the riblets is to impose an offset for the no-slip boundary condition which is further into the flow for the

spanwise velocity fluctuations than for the streamwise ones. They reasoned that this would move the quasi-streamwise vortices away from the wall, thickening the viscous sublayer and lowering the drag. They computed the relative offset $\Delta y/k$ for several riblet families and estimated that

$$\Delta U^+ \approx 0.8\Delta y^+, \quad (13)$$

assuming that the depth of the sublayer increases exactly by Δy . Jiménez (1994) carried out direct numerical simulations of turbulent channels incorporating the offset of the boundary conditions, and confirmed that all the transverse velocity fluctuations are shifted by Δy , obtaining a drag law $\Delta U^+ \approx 0.9\Delta y^+$. Actual riblets satisfy a linear law similar to Equation 13 with somewhat lower experimental slopes, which Bechert et al. (1997) showed to be due to the mechanical rounding of their tips. Because $\Delta y/k$ is constant for each riblet shape, this implies a linear behavior of the roughness function at low k^+ . This is faster than the quadratic one suggested by Bradshaw (2000), showing that there are roughness effects that go beyond simple aerodynamic drag. Luchini et al.'s (1991) argument and Jiménez's (1994) simulations are antisymmetric in Δy when $\Delta y \ll 1$, and imply that the drag of spanwise-mounted riblets should increase linearly with k^+ .

Colebrook (1939) suggested that the reason for the gradual buildup of the roughness effects in industrial surfaces is that they contain irregularities of different sizes, and that each element becomes active when it individually reaches a critical Reynolds number. The overall smooth evolution of the drag is the sum of these individual transitions. Colebrook & White (1937) provided some support for this model in a series of experiments in which they used sand grains of different sizes to roughen the wall. Well-graded sand led to results agreeing with Nikuradse (1933), but as little as 2.5% of larger grains were enough to substantially lengthen the transitional regime. The very sharp transition for the uniform tightly packed spheres included in Figure 3 also supports this model.

There is another interesting interpretation of Figure 3. Roughness has two effects in the transitional regime. In the first place it creates an extra form drag, which increases skin friction, but it also weakens the viscous generation cycle, which decreases it. The geometric offset in riblets is an example of the second effect, which is dominant in that case because the riblets, aligned with the mean flow, have little form drag. As k^+ increases, and the viscous cycle is completely destroyed, the savings from that effect saturate, and the form drag eventually takes over. Different surfaces in Figure 3 have different balances of both effects. In the case of surfaces with sparsely distributed roughness elements, the form drag increases before the viscous cycle is modified over most of the wall, and the savings are never realized. If this interpretation is correct, uniformly rough surfaces offer the best opportunity for drag-reducing roughness, and Figure 3 suggests that it would be interesting to extend the experiments on packed spheres to lower k^+ .

3. TURBULENCE STRUCTURE

Roughness has a profound influence on the turbulence structure in a layer whose depth is given by Raupach et al. (1991) as $k_R/k = 2-5$. Raupach & Tom (1981) found that below $k_R = k + D$, where D is the mean interelement separation, the turbulence properties depend on the location with respect to the roughness elements. In the limit of very large D/k Sabot et al. (1977) found $k_R/k \approx 4.5$ for a pipe with spanwise fences with $D/k = 10$. A working approximation used in the discussions below is

$$k_R/k = \min(1 + D/k, 5). \quad (14)$$

We define k in this article as the height of the roughness elements; other authors use the protrusion height of the elements above the virtual origin of the logarithmic layer. Some of the experiments mentioned below would have higher δ/k if the protrusion height had been used, but the difference is usually compensated by the influence of D .

The behavior of turbulence within the roughness layer depends too much on the details of the surface to be reviewed here. A more interesting question is whether some roughness effects extend above k_R and into the outer layer even when δ/k_R is large. That would tell a lot about the interactions between the inner and outer layers, and in particular about whether the latter is controlled by the former. The “classical” answer is summarized in Figure 4, which displays spectra of the streamwise velocity in a smooth and in a rough pipe ($\delta/k \approx 200$). Each horizontal line is a premultiplied spectrum normalized to unit energy, and they are stacked to form single functions of y and of the streamwise wavelength. The smooth and rough spectra agree above $y/R \approx 0.15$ ($y/k_R \approx 6$), and the same is true of most other properties of the turbulent fluctuations.

3.1. Length Scales

The strongest challenge has come from Krogstad et al. (1992) and Krogstad & Antonia (1994). They found that the one-point correlation times for all the velocity components, $U_\delta T/\delta$, are about twice shorter for rough than for smooth boundary layers below $y/\delta < 0.5$. Although the height of their mesh roughness, $\delta/k \approx 50$ ($\delta/k_R \approx 20$, $\Delta U^+ = 11$), is marginal according to the criteria developed above, it is a little too large to dismiss the results on those grounds.

That observation has attracted a lot of interest, but it has been difficult for other investigators to reproduce it. Krogstad et al. (1992) and Krogstad & Antonia (1999) published frequency spectra for u and v over the same rough wall used by Krogstad & Antonia (1994), and there is little difference in the positions of their smooth and rough spectral peaks at $y/\delta = 0.4-0.5$. The correlation time is only indirectly related to the spectral peak, but this disagreement suggests that

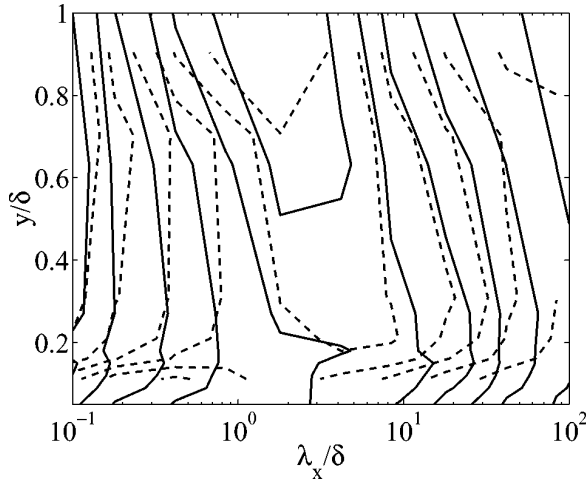


Figure 4 Premultiplied spectral density $k_x E_{uu}$, as a function of the streamwise wavelength $\lambda_x = 2\pi/k_x$, and of the wall distance (Perry & Abell 1977). —, smooth wall; ---, rough wall.

the differences between rough and smooth flows are not associated with the most energetic velocity structures.

Nakagawa & Hanratty (2001) studied a channel over two-dimensional sinusoidal roughness ($\delta/k \approx 60$, $\Delta U^+ = 9$), and found correlation lengths, L/δ , which are equal to those in smooth channels. Sabot et al. (1977) studied a very rough pipe with spanwise fences ($\delta/k = 15$, $\Delta U^+ = 17$) and found that the streamwise integral lengths for u and v change little with roughness. Comparing correlation lengths with times requires choosing an advection velocity, which changes both with the wavelength and with the distance to the wall (Krogstad et al. 1998). The question is not trivial, and the ratio between the smooth and rough times in Krogstad & Antonia (1994) varies between 1.6 and 2.5 depending on whether they are normalized with the friction, free-stream, or local velocities. The advection velocity also changes from rough to smooth flows, as a natural consequence of modifying the mean velocity profile. For example, Sabot et al. (1977) found that the advection velocity of the large scales is 1.3 times faster in their smooth pipe than in the rough one. However, none of these corrections is enough to fully account for the observed differences in the correlation times.

Krogstad & Antonia (1994) also measured the inclination angle of the two-point correlation function of u between two y locations. They obtain 38° in the rough case against 10° in the smooth one. This disagreement is not as worrying as the one discussed above because it is done fairly near the roughness layer ($y/k_R \approx 3$) and may be a local effect, but Nakagawa & Hanratty (2001) found no change in this quantity. Because they used particle image velocimetry (PIV),

which is a purely spatial procedure, they suggested that their disagreement with Krogstad & Antonia (1994) may be due to the previously discussed ambiguity of the advection velocity. Using different assumptions on the velocities reduces the angle to about 25° which, while still high, is closer to the smooth one. Because of these experimental uncertainties, and because of the marginal value of δ/k in all these cases, the claim of large changes in the length scales above the roughness layer requires further confirmation.

3.2. Wake Intensity

Another indication of the effect of the roughness on the outer part of the boundary layer is its effect on the wake parameter Π . The classical result is again that Π changes little between rough and smooth boundary layers at the same Reynolds number (Hama 1954, Clauser 1956), but later authors reported substantial deviations. One problem is how to define Π in flows without a well-defined logarithmic layer, such as those with low δ^+ or δ/k , and the results from different investigators are not always comparable.

Tani (1987) reviewed several data sets using a uniform analysis scheme, and the conclusion from his work is that most differences are due to low values of δ/k . Although for several k -surfaces he found $\Pi \approx 0\text{--}0.8$ when $\delta/k < 60$, they all tend to $\Pi \approx 0.45$ when $\delta/k > 100$. This is close to the value $\Pi \approx 0.52$ for smooth walls (Fernholz & Finley 1996).

D -type surfaces are more interesting in this respect because the claim that their roughness length scale is proportional to the boundary-layer thickness suggests that the effect of the roughness might be felt throughout the layer. Tani (1987) compiled some of those cases and found $\Pi = 0.6\text{--}0.7$ for all of them, which is higher than the smooth-wall value, although only the data from Bandyopadhyay (1987) have $\delta/k \gtrsim 100$. As with most available results for d -roughness, this one is tantalizing but requires confirmation.

3.3. Velocity Fluctuations Intensities

The intensity of the velocity fluctuations is measured in most roughness experiments, and is a lowest-order indicator of the wall's influence on other parts of the flow. Consider the streamwise fluctuation profiles in Figure 5. As k_s^+ increases and the form drag dominates over the viscous one, the near-wall peak in u' disappears, and the profiles develop a maximum in the logarithmic layer around $y/\delta = 0.05\text{--}0.2$. This outer peak is probably the same as the plateau found in that region for high Reynolds number flows over smooth walls, whose intensity was shown by DeGraaff & Eaton (2000) to scale best in the mixed units used in Figure 6a. For rough walls this scaling also works reasonably well, but there is an additional increase with k_s^+ , and probably also with δ/k . The flows in the higher "branch" in Figure 6a have $\delta/k \gtrsim 80$. The presence of the free-stream velocity U_δ in the scaling of the streamwise fluctuations is usually associated with the effect of the inactive motions postulated by Townsend (1976), although the details of

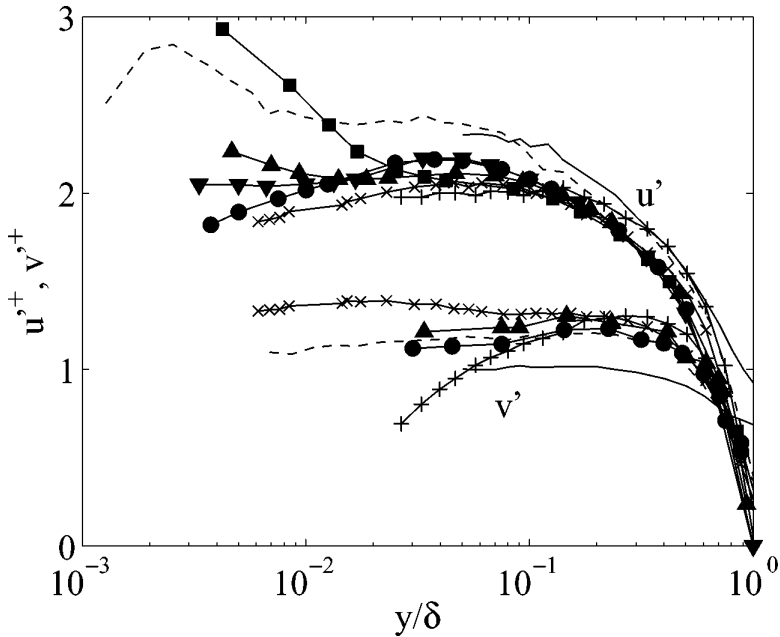


Figure 5 Streamwise and wall-normal r.m.s. velocity fluctuations against y/δ . +, Spanwise rods. $\delta/k = 30, k_s^+ = 253$; \times , woven mesh. $\delta/k = 56, k_s^+ = 345$ (Krogstad & Antonia 1999); \blacksquare , $k_s^+ \approx 21$; \blacktriangle , $k_s^+ \approx 35$; \blacktriangledown , $k_s^+ \approx 45$; \bullet , $k_s^+ \approx 62$; $\delta/k \approx 80$. Closely packed spheres (Ligrani & Moffat 1986); - - -, smooth boundary layer. $\delta^+ = 7300$ (Fernholz et al. 1995); —, smooth pipe. $\delta^+ = 3900$ (Perry, Henbest & Chong 1986).

how they affect the fluctuations away from the wall layer are not well understood. The same explanation would be reasonable in the case of k_s^+ because roughness will likely generate “sterile” turbulence with no Reynolds stress, but it is also unclear how the effect leaks outside the roughness layer. Figure 5 includes profiles for the wall-normal fluctuations. The effect of the roughness is weaker for this quantity, which has no near-wall peak over smooth surfaces, and the plateau in the logarithmic layer changes little from the smooth to the rough flows. The strong damping of the fluctuations over the spanwise rods of Krogstad & Antonia (1999) occurs below $y = 3k$. There is a weak decreasing trend with k_s^+ , which may be spurious, but once the fully rough regime is reached there is little evidence for a dependence on δ/k . This agrees with the lack of Reynolds number dependence of v'^+ over smooth walls (DeGraaff & Eaton 2000). Part of the scatter in the maximum intensities in Figure 6b can be explained by separating them into boundary layers and pipes or channels. Both groups are relatively homogeneous, at least for $\delta/k > 20$, but distinct. The maximum v' is 20% lower in pipes than in boundary layers, but this is also true for flows over smooth walls, two of which are included in Figure 5. This difference between internal and external flows is interesting, and

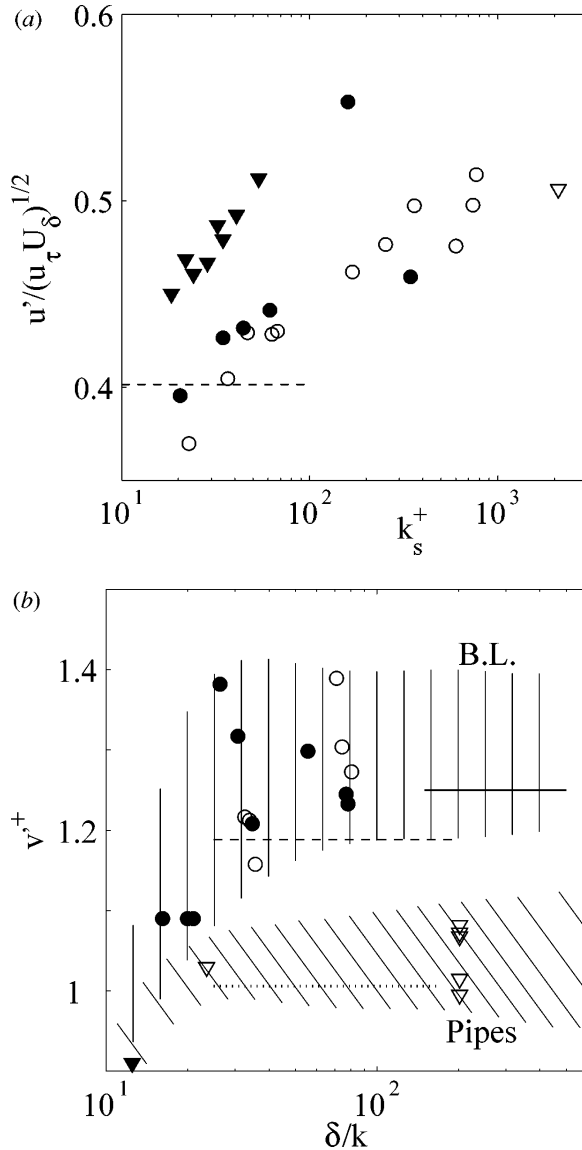


Figure 6 R.m.s. velocity fluctuations from various sources. \circ , rough boundary layers; ∇ , rough pipes or channels; ----, smooth boundary layers (DeGraaff & Eaton 2000); —, atmospheric boundary layer (Panofsky 1974, Counihan 1975); ·····, smooth pipes (Perry et al. 1986). (a) u' at $y/\delta = 0.1$. Solid symbols have $\delta/k > 50$. (b) Maximum of v' . Solid symbols have $k_s^+ > 50$.

suggests that there are v -structures that span the whole boundary-layer thickness and feel the outer-edge conditions. A possible mechanism for this difference is the wall-normal transport of turbulent energy, which in smooth channels is carried by turbulent diffusion and takes excess energy produced by the near-wall cycle to be dissipated in the core layer (Jiménez 1999). In boundary layers the extra energy is used to sustain the thickening of the layer, and part of the flux is carried by the mean wall-normal velocity. Rough flows promise to add to this diversity by changing the balance between production and dissipation in the roughness layer, and therefore the magnitude of the exported flux. However, the experimental evidence is contradictory. Whereas some experimenters find fluxes that agree with the smooth value, even if the fluctuation profiles change (Raupach 1981, Krogstad & Antonia 1999), others find the same fluctuation profiles with very different energy fluxes (Keirsbulck et al. 2002). It is not clear whether this is due to the experimental difficulty of measuring the energy flux, whether it means that the fluctuations are insensitive to it, or whether it is simply a consequence of trying to understand a complex phenomenon from very few experiments. It would be desirable for future experiments and computations to look at this quantity in more detail.

4. THEORETICAL MODELS

Numerical simulations, which have done so much to clarify other areas of turbulence, have still not left their mark on the understanding of rough-walled flows. There are numerous modifications to Reynolds-averaged simulation models that include roughness effects (Patel 1998, Durbin et al. 2001), but they are a posteriori applications of physical insight that are beyond our scope. From the point of view of a priori simulations the problem is computational cost. To be reasonably free from direct roughness effects we need $\delta/k \gtrsim 50$, and to have well-developed roughness we should have $k^+ \gtrsim 80$. To have a well-defined rough turbulent flow that is neither transitional in the sense of low k^+ , nor of insufficient boundary-layer thickness, we therefore need $\delta^+ \gtrsim 4000$. The largest direct simulations of wall-bounded flows have at present $\delta^+ \approx 2000$. Large-eddy simulations could help in raising the Reynolds number, but they imply modeling the small scales, which is dangerous when trying to clarify the effect of small-scale roughness. Direct simulations limited in one of the two parameters just mentioned are beginning to appear in conferences, and some of them will probably be published at the time of this review's publication (Bhaganagar & Kim 2002, Lee 2002, Leonardi et al. 2002, Nozawa et al. 2002). Direct simulations of the flow over riblets, in which the regime of interest is that of transitional k^+ , have been available for some time (Chu & Karniadakis 1993, Choi et al. 1993, Goldstein et al. 1995), but they also have low δ/k . In all these cases the emphasis is on the exact representation of the flow over the roughness elements, and on the details of the flow within the roughness layer. An alternative approach, which has to be applied with care because it involves modeling, but which bypasses some of the limitations of strict direct simulations, is to substitute the effect of the roughness layer by an "equivalent" wall-boundary condition. Low- k^+ riblets can be substituted by an offset between

the locations of the streamwise and spanwise no-slip conditions. If we choose our origin at the no-slip position for u , and assume that the instantaneous velocity profile stays linear near the wall, we can write this as

$$w(x, 0, z) + \alpha \partial_y w(x, 0, z) = 0, \quad (15)$$

where α is an adjustable parameter. Choi et al. (1993) used boundary conditions of this type as control devices to manipulate the skin friction in channel flows, obtaining changes in the drag coefficient of the order of $\pm 50\%$ ($k_s^+ \approx \pm 60$). Jiménez et al. (2001) used mixed boundary conditions that can be put in the form of Equation 15 for the wall-normal velocity to model the effect of a perforated wall. There is also in that case a large increase in the skin friction, which was traced to the appearance of large-scale instabilities of the mean velocity profile, in the form of large spanwise structures essentially spanning the full boundary-layer thickness. They originate from a lightly damped linear mode of the mean velocity profile over an impermeable wall, and connect to the Kelvin-Helmholtz instability of inflectional profiles in the limit of infinite permeability. Finnigan (2000) invoked similar inflectional instabilities to explain the properties of the roughness layer above plant canopies. It is interesting that such models generate effects similar to those of roughness without considering the details of the individual roughness elements, and that they produce length scales which are only linked to averaged properties of the wall. This brings to mind d -rough behavior, where the scale of the structures is determined by the boundary-layer properties instead of by the surface geometry. Although the details are beyond the space available in this review, it is possible to devise artificial boundary conditions of the type of Equation 15 for v that arise naturally as approximations of the flow along the grooves of a d -wall under the effect of spanwise pressure gradients. Their stability has not been studied in detail but, in simple inviscid cases, they lead to instabilities of the mean flow for which the most unstable eigenmodes are large streamwise velocity streaks. The flow over rough walls is generally too complicated to sustain streaks like the ones found over smooth walls, but Liu et al. (1966) and Djenidi et al. (1999) observed longitudinal streaks over d -surfaces. No direct simulations exist of fully turbulent flows with averaged boundary conditions designed to mimic high- k^+ directional wall roughness, but considerations such as the ones above suggest that they could help to clarify the dynamics of rough-wall turbulence in general, and of d -roughness in particular.

5. SUMMARY AND CONCLUSIONS

The effect of rough walls on turbulent boundary layers is controlled by two dimensionless parameters. The roughness Reynolds number, k_s^+ or ΔU^+ , quantifies the extent of the interference of the roughness with the buffer layer. The transitionally rough regime in which $k_s^+ \lesssim 50$ is highly variable, with behaviors ranging from the gradual transitions of irregular surfaces, to the sharper ones in more uniform geometries, or even to the drag reduction by riblets.

A second parameter, whose importance has always been explicitly recognized, but that has been somewhat neglected lately, is the blockage ratio δ/k of the boundary-layer thickness to the roughness height. It measures the direct effect of the roughness on the logarithmic layer, where most of the energy production and the mean shear are concentrated. Elementary considerations suggest that δ/k has to be larger than 40 before similarity laws can be expected, and experimental results suggest that the threshold is closer to $\delta/k \approx 80$. Flows with higher blockage fractions retain few of the mechanisms of normal wall turbulence, and can better be described as flows over obstacles. They are also very dependent on the roughness geometry.

The main conclusion from the part of this review dedicated to turbulent structure is that the matter is far from being understood. There are conflicting experiments in almost all cases and, even for those quantities for which the trends are clear, the data collapse is poor. This is in part due to the industrial emphasis of many experimental investigations, which do not probe into the structure of the flow. Also part of the problem is the variety of rough surfaces, which strongly influence the dynamics of the roughness layer. But we should be able to say something about the nature of the high δ/k limit, in which the effect of the roughness presumably reaches the outer flow only after a long series of chaotic interactions.

The classical result is that the buffer layer can be perturbed without transmitting to the outer flow anything beyond a change in skin friction, but there are indications of deeper interactions. The increase of u' in the logarithmic region is clear, and seems to survive as δ/k increases, but others, such as the changes in length scales, are contaminated by experimental issues and by marginal blockage. If confirmed, they would have implications beyond the study of roughness itself. For example, large-eddy simulation is based on the idea that there is little information flowing from the small to the large scales, and identifying a backscatter mechanism stretching across the boundary layer would complicate the modeling of wall-bounded flows considerably.

What is needed to clarify this matter is a well-characterized set of experiments in which both k^+ and δ/k are large enough to be free from transitional effects. The experimental or numerical study of asymptotic roughness is challenging because the product of k^+ and δ/k is the Reynolds number of the flow. If both quantities are reasonably high, δ^+ has to be at least 4000. The tendency in the past decade has been to concentrate on the fully rough regime at comparatively low δ/k . In the absence of the asymptotic experiments mentioned above, the results in this review suggest that the opposite limit of transitionally rough flows with high δ/k would also be rewarding.

ACKNOWLEDGMENTS

The preparation of this review was supported in part by the CICYT grant BFM 2000-1468. I am grateful to numerous colleagues who have provided original data, publications, and discussions, but especially to R.A. Antonia, P-A. Krogstad, H. Nagib, and to the late A.E. Perry.

The Annual Review of Fluid Mechanics is online at <http://fluid.annualreviews.org>

LITERATURE CITED

- Adrian RJ, Meinhart CD, Tomkins CD. 2000. Vortex organization in the outer region of the turbulent boundary layer. *J. Fluid Mech.* 422:1–54
- Bandyopadhyay PR. 1987. Rough-wall turbulent boundary layers in the transition regime. *J. Fluid Mech.* 180:231–66
- Bandyopadhyay PR, Watson RD. 1988. Structure of rough-wall turbulent boundary layers. *Phys. Fluids* 31:1877–83
- Barenblatt GI, Chorin AJ. 1998. Scaling of the intermediate region in wall-bounded turbulence: The power law. *Phys. Fluids* 10:1043–44
- Bechert DW, Bruse M, Hage W. 2000. Experiments with three-dimensional riblets as an idealized model of shark skin. *Exp. Fluids* 28:403–12
- Bechert DW, Bruse M, Hage W, Van der Hoeven JGT, Hoppe G. 1997. Experiment on drag-reducing surfaces and their optimization with an adjustable geometry. *J. Fluid Mech.* 338:59–87
- Bhaganagar K, Kim J. 2002. Physics of rough-wall turbulent boundary layer. *Bull. Am. Phys. Soc.* 47(10):55
- Bradshaw P. 2000. A note on “critical roughness” height and “transitional roughness.” *Phys. Fluids* 6:1611–14
- Chen H, Castro IP. 2002. Near-wall flow over urban-like roughness. *Boundary-layer Meteorol.* 104:229–59
- Choi H, Moin P, Kim J. 1993. Direct numerical simulation of turbulent flow over riblets. *J. Fluid Mech.* 255:503–39
- Choi H, Moin P, Kim J. 1994. Active turbulence control and drag reduction in wall-bounded flows. *J. Fluid Mech.* 262:75–110
- Chu DC, Karniadakis GE. 1993. A direct numerical simulation of laminar and turbulent flow over riblet-mounted surfaces. *J. Fluid Mech.* 250:1–42
- Clauser FH. 1956. The turbulent boundary layer. *Adv. Appl. Mech.* 4:1–51
- Colebrook CF. 1939. Turbulent flow in pipes with particular reference to the transition region between the smooth- and rough-pipe laws. *J. Inst. Civil Eng.* 11:133–56
- Colebrook CF, White CM. 1937. Experiments with fluid friction in roughened pipes. *Proc. R. Soc. London Ser. A* 161:367–81
- Coleman HW, Hodge BK, Taylor RP. 1984. A re-evaluation of Schlichting’s surface roughness experiment. *J. Fluids Eng.* 106:60–65
- Counihan J. 1975. Adiabatic atmospheric boundary layers: A review and analysis of data from the period 1880–1972. *Atmos. Environ.* 9:871–905
- Darcy H. 1857. *Recherches expérimentales relatives au mouvement de l’eau dans les tuyaux*. Paris: Mallet-Bachelier. 268 pp.
- DeGraaff DB, Eaton JK. 2000. Reynolds-number scaling of the flat-plate turbulent boundary layer. *J. Fluid Mech.* 422:319–46
- Del Álamo JC, Jiménez J. 2003. Spectra of the very large scales in turbulent channels. *Phys. Fluids* 15:41–44
- Djenidi L, Anselmetti F, Antonia RA. 1994. LDA measurements in a turbulent boundary layer over a *d*-type rough wall. *Exp. Fluids* 16:323–29
- Djenidi L, Elavarasan R, Antonia RA. 1999. The turbulent boundary layer over transverse square cavities. *J. Fluid Mech.* 395:271–94
- Durbin PA, Medic G, Seo J-M, Eaton JK, Song S. 2001. Rough wall modification of two-layer *k-ε*. *J. Fluids Eng.* 123:16–21
- Dvorak FA. 1969. Calculation of turbulent boundary layers on rough surfaces in pressure gradient. *AIAA J.* 7:1752–59
- Fernholz HH, Finley PJ. 1996. The incompressible zero-pressure-gradient turbulent boundary layer: an assessment of the data. *Prog. Aerospace Sci.* 32:245–311
- Fernholz HH, Krause E, Nockermann M,

- Schober M. 1995. Comparative measurements in the canonical boundary layer at $Re_{\delta_2} \leq 6 \times 10^4$ on the wall of the German-Dutch wind tunnel. *Phys. Fluids* 7:1275–81
- Finnigan J. 2000. Turbulence in plant canopies. *Annu. Rev. Fluid Mech.* 32:519–71
- Ghaddar NK, Korczak KZ, Mikic BB, Patera AT. 1986a. Numerical investigation of incompressible flow in grooved channels. Part 1. Stability and self-sustained oscillations. *J. Fluid Mech.* 163:99–127
- Ghaddar NK, Magen M, Mikic BB, Patera AT. 1986b. Numerical investigation of incompressible flow in grooved channels. Part 2. Resonance and oscillatory heat-transfer enhancement. *J. Fluid Mech.* 168:541–67
- Goldstein D, Handler R, Sirovich L. 1995. Direct numerical simulation of turbulent flow over modelled riblet-covered surface. *J. Fluid Mech.* 302:333–76
- Hagen G. 1854. Über den Einfluss der Temperatur auf die Bewegung des Wassers in Röhren. *Math. Abh. Akad. Wiss. Berlin*, pp. 17–98
- Hama FR. 1954. Boundary layer characteristics for smooth and rough surfaces. *Trans. Soc. Naval Archit. Mar. Eng.* 62:333–58
- Hamilton JM, Kim J, Waleffe F. 1995. Regeneration mechanisms of near-wall turbulence structures. *J. Fluid Mech.* 287:317–48
- Head MR, Bandyopadhyay P. 1981. New aspects of turbulent boundary-layer structure. *J. Fluid Mech.* 107:297–338
- Hites MH. 1997. *Scaling of high-Reynolds number turbulent boundary layers in the National Diagnostic Facility*. PhD. thesis. Ill. Inst. Technol.
- Hutchings IM. 1992. *Tribology: Friction and Wear of Engineering Materials*, pp. 4–15. London: Arnold
- Jiménez J. 1994. On the structure and control of near wall turbulence. *Phys. Fluids* 6:944–53
- Jiménez J. 1999. The physics of wall turbulence. *Physica A* 263:252–62
- Jiménez J, Moin P. 1991. The minimal flow unit in near wall turbulence. *J. Fluid Mech.* 225:221–40
- Jiménez J, Pinelli A. 1999. The autonomous cycle of near-wall turbulence. *J. Fluid Mech.* 389:335–59
- Jiménez J, Uhlmann M, Pinelli A, Kawahara G. 2001. Turbulent shear flow over active and passive porous surfaces. *J. Fluid Mech.* 442:89–117
- Kalinin EK, Dreitzer GA. 1998. Heat transfer enhancement in heat exchangers. *Adv. Heat Transf.* 31:159–332
- Keirsbulck L, Labraga L, Mazouz A, Tournier C. 2002. Surface roughness effects on turbulent boundary layer structures. *J. Fluids Eng.* 124:127–35
- Krogstad P-A, Antonia RA. 1994. Structure of turbulent boundary layers on smooth and rough walls. *J. Fluid Mech.* 277:1–21
- Krogstad P-A, Antonia RA. 1999. Surface roughness effects in turbulent boundary layers. *Exp. Fluids* 27:450–60
- Krogstad P-A, Antonia RA, Browne LWB. 1992. Comparison between rough- and smooth-wall turbulent boundary layers. *J. Fluid Mech.* 245:599–617
- Krogstad P-A, Kaspersen JH, Rimestad S. 1998. Convection velocities in turbulent boundary layers. *Phys. Fluids* 10:949–57
- Laufer J, Narayanan MAB. 1971. Mean period of the turbulent production mechanism in a boundary layer. *Phys. Fluids* 14:182–83
- Lee C. 2002. Direct numerical simulations of rough-wall channel flows. *Bull. Am. Phys. Soc.* 47(10):111
- Leonardi S, Orlandi P, Djenidi L, Antonia RA. 2002. DNS of a turbulent channel flow with different rough walls, In *Advances in Turbulence IX*, ed. IP Castro, PE Hancock, TG Thomas, pp. 387–90. Barcelona: CIMNE
- Ligrani PM, Moffat RJ. 1986. Structure of transitionally rough and fully rough turbulent boundary layers. *J. Fluid Mech.* 162:69–98
- Liou T-M, Chang Y, Hwang D-W. 1990. Experimental and computational study of turbulent flows in a channel with two pairs of turbulence promoters in tandem. *J. Fluid Eng.* 112:302–10
- Liu CK, Kline SJ, Johnston JP. 1966. An experimental study of turbulent boundary layers on

- rough walls. *Rep. MD-15*. Thermosci. Div., Stanford Univ.
- Luchik TS, Tiederman WG. 1987. Timescale and structure of ejections in turbulent channel flows. *J. Fluid Mech.* 174:529–52
- Luchini P, Manzo F, Pozzi A. 1991. Resistance of a grooved surface to parallel flow and cross-flow. *J. Fluid Mech.* 228:87–109
- Monin AS. 1970. The atmospheric boundary layer. *Annu. Rev. Fluid Mech.* 2:225–50
- Moody LF. 1944. Friction factors for pipe flow. *Trans. ASME* 66:671–84
- Nakagawa S, Hanratty TJ. 2001. Particle image velocimetry measurements over a wavy wall. *Phys. Fluids* 13:3504–7
- Nikuradse J. 1933. Strömungsgesetze in Rauhen Rohren, *VDI-Forsch.* 361 (Engl. transl. 1950. Laws of flow in rough pipes. *NACA TM 1292*)
- Nozawa K, Tamura T, Cao S. 2002. LES study on streamwise spatial variation of turbulence structures in rough-wall boundary layer. *Bull. Am. Phys. Soc.* 47(10):55–56
- Panofsky HA. 1974. The atmospheric boundary layer below 150 meters. *Annu. Rev. Fluid Mech.* 6:147–77
- Patel VC. 1998. Perspective: flow at high Reynolds number and over rough surfaces—Achilles heel of CFD. *J. Fluids Eng.* 120: 434–44
- Perry AE, Abell CJ. 1977. Asymptotic similarity of turbulence structures in smooth- and rough-walled pipes. *J. Fluid Mech.* 79:785–99
- Perry AE, Hafez S, Chong MS. 2001. A possible reinterpretation of the Princeton super-pipe data. *J. Fluid Mech.* 439:395–401
- Perry AE, Henbest S, Chong MS. 1986. A theoretical and experimental study of wall turbulence. *J. Fluid Mech.* 165:163–199. Case PCH02 in “A selection of test cases for the validation of large-eddy simulations of turbulent flows.” *AGARD Adv. Rep.* 345
- Perry AE, Schofield WH, Joubert P. 1969. Rough wall turbulent boundary layers. *J. Fluid Mech.* 37:383–413
- Raupach MR. 1981. Conditional statistics of Reynolds stress in rough-wall and smooth-wall turbulent boundary layers. *J. Fluid Mech.* 108:363–82
- Raupach MR, Antonia RA, Rajagopalan S. 1991. Rough-wall turbulent boundary layers. *Appl. Mech. Rev.* 44:1–25
- Raupach MR, Tom AS. 1981. Turbulence in and above plant canopies. *Annu. Rev. Fluid Mech.* 13:97–129
- Robinson SK. 1991. Coherent motions in the turbulent boundary layer. *Annu. Rev. Fluid Mech.* 23:601–39
- Sabot J, Saleh I, Comte-Bellot G. 1977. Effect of roughness on the intermittent maintenance of Reynolds shear stress in pipe flow. *Phys. Fluids* 20:S150–55
- Scaggs WF, Taylor RP, Coleman HW. 1988. Measurement and prediction of rough wall effects on friction factor—Uniform roughness results. *J. Fluid Eng.* 110:385–91
- Schlichting H. 1936. Experimentelle Untersuchungen zum Rauheitsproblem. *Ing. Arch.* 7:1–34. (Engl. transl. 1937. Experimental investigation of the problem of surface roughness. *NACA TM 823*)
- Schlichting H. 1968. *Boundary Layer Theory*. New York: McGraw-Hill. 747 pp. 6th ed.
- Shah DA, Antonia RA. 1989. Scaling of the bursting period in turbulent boundary layer and duct flow. *Phys. Fluids* A1:318–25
- Simpson RL. 1973. A generalized correlation of roughness density effects on the turbulent boundary layer. *AIAA J.* 11:242–44
- Sirovich L, Karlsson S. 1997. Turbulent drag reduction by passive mechanisms. *Nature* 388:753–55
- Tani I. 1987. Turbulent boundary layer development over rough surfaces. In *Perspectives in Turbulence Studies*, ed. HU Meier, P Bradshaw, pp. 223–49. Berlin: Springer-Verlag
- Tani I. 1988. Drag reduction by riblet viewed as a roughness problem. *Proc. Jpn. Acad. B* 64:21–24
- Taniguchi Y, Evans JW. 1993. Some measurements of the penetration of turbulence into small cavities. *Int. J. Heat Mass Transf.* 36:961–65

- Taylor RP, Coleman HW, Hodge BK. 1985. Prediction of turbulent rough-wall skin friction using a discrete element approach. *J. Fluid Eng.* 107:251–57
- Tillman W. 1944. Neue Widerstandsmessungen an Oberflächenstörungen in der turbulenten Reibungsschicht, *ZWB Untersuch. Mitteil.* 6619 (Engl. transl. 1951. Additional measurements of the drag of surface irregularities in turbulent boundary layers. *NACA TM 1299*)
- Townsend AA. 1976. *The Structure of Turbulent Shear Flows*. Cambridge, UK: Cambridge Univ. Press. 429 pp. 2nd ed.
- Townsin RL. 1991. The correlation of added drag with surface roughness parameters. In *Recent Developments in Turbulence Management*, ed. K-S Choi, pp. 181–91. Amsterdam: Kluwer
- Waigh DR, Kind RJ. 1998. Improved aerodynamic characterization of regular three-dimensional roughness. *AIAA J.* 36:1117–19
- Walsh MJ. 1990. Riblets. In *Viscous Drag Reduction in Boundary Layers*, ed. DM Bushnell, JN Hefner, pp. 203–61. New York: AIAA
- Wassermann P, Kloker M. 2002. Mechanisms and passive control of crossflow-vortex-induced transition in a three-dimensional boundary layer. *J. Fluid Mech.* 456: 49–84
- Webb RL, Eckert ERG, Goldstein RJ. 1971. Heat transfer and friction in tubes with repeated-rib roughness *Int. J. Heat Mass Transf.* 14:601–17
- White FM. 1991. *Viscous Fluid Flow*. New York: McGraw-Hill. 614 pp. 2nd ed.
- Wood DH, Antonia RA. 1975. Measurements in a turbulent boundary layer over a *d*-type surface roughness. *J. Appl. Mech.* 42:591–97